On the fast adaptive Fokker-Planck solver for fiber orientation dynamics in turbulent carrier flows

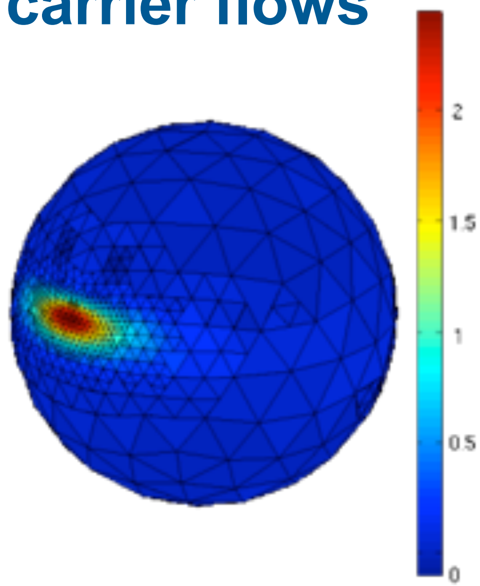

Evgeniy Zharovsky
zharovsk@ma.tum.de

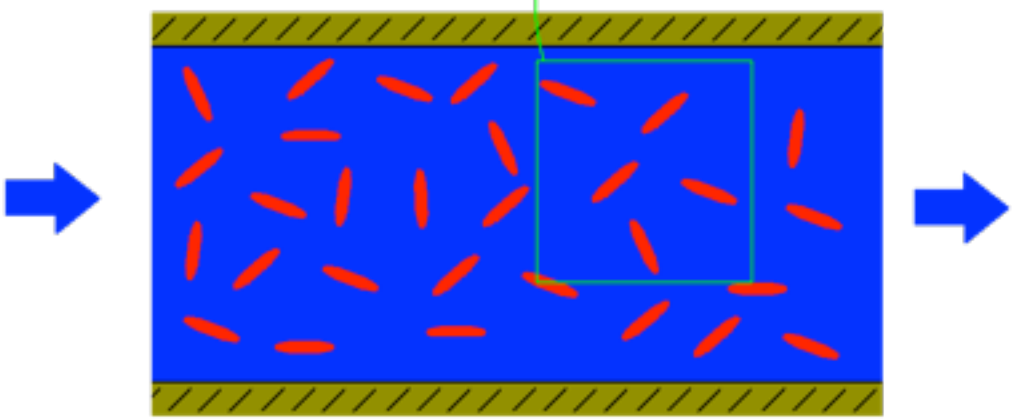

Outline

- Applications: fiber laden flows
- The model
- Numerical scheme
    - Geodesic grids
    - Adaptivity
- Tests and Results
- Conclusion
- Acknowledgement

Applications: fiber laden flows

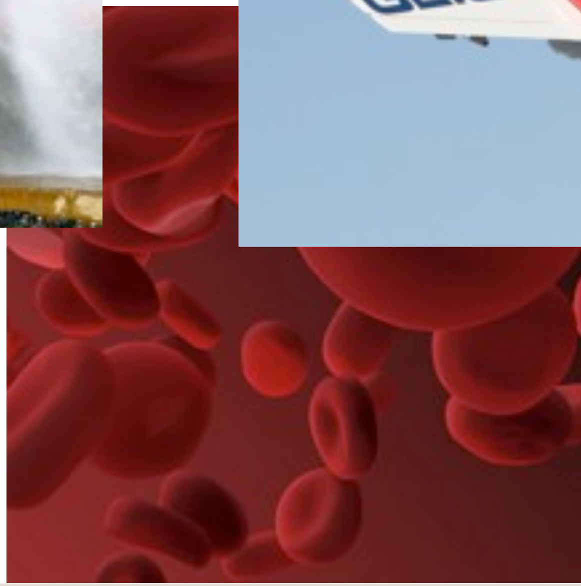

Why turbulent flows?

Why turbulent flows?

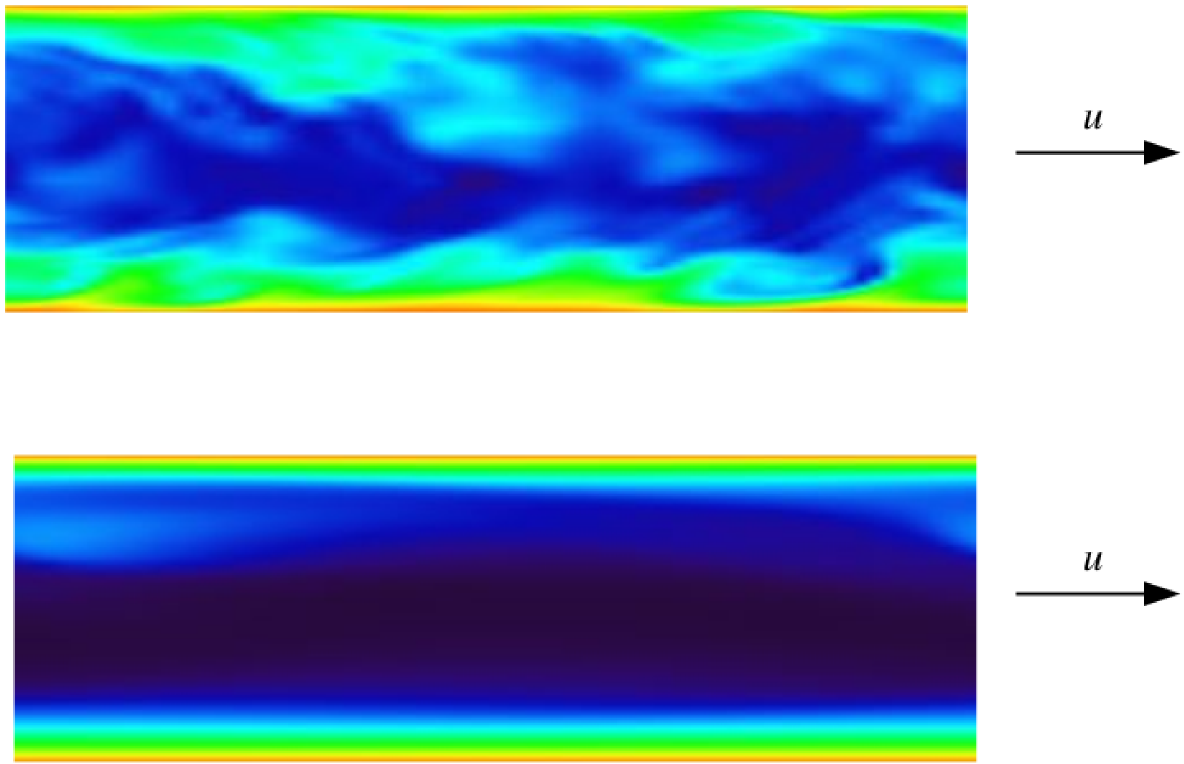

figures by Manhart

The model

Orientation description

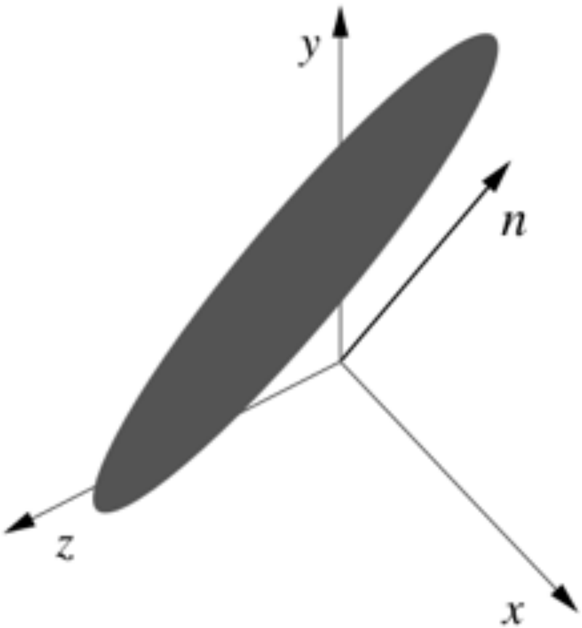

$$\|\mathbf{n}\| = 1$$

$$\Leftrightarrow$$

$$\mathbf{n} \in \partial B(0;1)$$

Orientation description

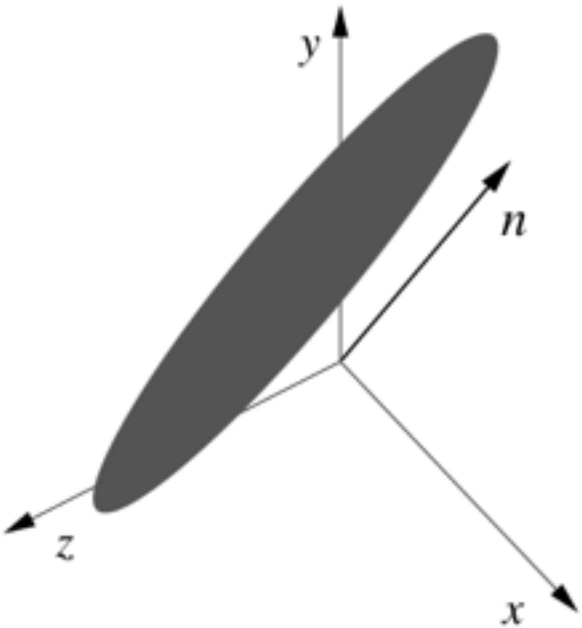

$$\|\mathbf{n}\| = 1$$

$$\Leftrightarrow$$

$$\boxed{\mathbf{n} \in \partial B(0;1)}$$

TECHNISCHE UNIVERSITÄT MÜNCHEN

Orientation dynamics (Fokker-Planck)

$$\partial_t \Psi = -\nabla_{\mathbf{n}} \cdot \left(\Psi \mathbf{f}(\mathbf{n}, t)\right) + D_r \Delta_{\mathbf{n}} \Psi$$

Orientation dynamics (Fokker-Planck)

$$\partial_t \Psi = -\nabla_{\mathbf{n}} \cdot (\Psi \mathbf{f}(\mathbf{n}, t)) + D_r \Delta_{\mathbf{n}} \Psi$$

Ψ : stochastic density of the orientation probability

$\mathbf{f}(\mathbf{n}, t)$: Jeffery's equation

D_r : rotational diffusion coefficient $\left(= \frac{\dot{\gamma}}{Pe} \right)$

Jeffery's equation

$$\mathbf{f}(\mathbf{x},\mathbf{n},t) = \mathbf{\Omega}(\mathbf{x},t)\cdot\mathbf{n} + \kappa\left(\mathbf{D}(\mathbf{x},t)\cdot\mathbf{n} - (\mathbf{n}\cdot\mathbf{D}(\mathbf{x},t)\cdot\mathbf{n})\,\mathbf{n}\right)$$

Jeffery's equation

$$\mathbf{f}(\mathbf{x},\mathbf{n},t) = \boldsymbol{\Omega}(\mathbf{x},t)\cdot\mathbf{n} + \kappa\left(\mathbf{D}(\mathbf{x},t)\cdot\mathbf{n} - (\mathbf{n}\cdot\mathbf{D}(\mathbf{x},t)\cdot\mathbf{n})\,\mathbf{n}\right)$$

$$\boldsymbol{\Omega} = \frac{1}{2}\left(\nabla_{\mathbf{x}}\mathbf{u} - \nabla_{\mathbf{x}}\mathbf{u}^T\right) \qquad \mathbf{D} = \frac{1}{2}\left(\nabla_{\mathbf{x}}\mathbf{u} + \nabla_{\mathbf{x}}\mathbf{u}^T\right) \qquad \kappa = \frac{r^2-1}{r^2+1}$$

vorticity tensor

rate-of-strain tensor

r : aspect ratio

Orientation dynamics (Fokker-Planck)

$$\partial_t \Psi = -\nabla_{\mathbf{n}} \cdot \left(\Psi \mathbf{f}(\mathbf{n}, t) \right) + D_r \Delta_{\mathbf{n}} \Psi$$

convection-diffusion problem
(convection dominates)

The model

$$\nabla \cdot \boldsymbol{u} = 0$$

$$\rho \frac{D\boldsymbol{u}}{Dt} = -\nabla p + \nabla \cdot \boldsymbol{\tau}^{\mathrm{N}}$$

- Newtonian incompressible carrier fluid

The model

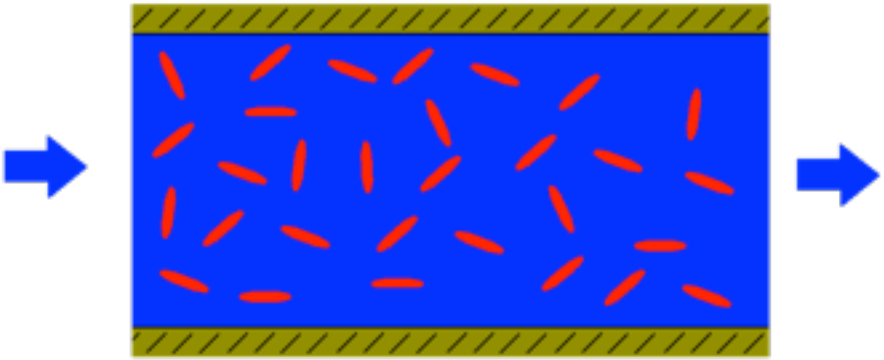

$$\nabla \cdot \boldsymbol{u} = 0$$

$$\rho \frac{D\boldsymbol{u}}{Dt} = -\nabla p + \nabla \cdot (\boldsymbol{\tau}^{\mathrm{N}} + \boldsymbol{\tau}^{\mathrm{NN}})$$

- Newtonian incompressible carrier fluid
- laden with small particles

Non-Newtonian stress (Batchelor,Brenner)

$$\boldsymbol{\tau}^{\mathrm{NN}} = \boldsymbol{\tau}^{\mathrm{NN}}(\Psi)$$

Non-Newtonian stress (Batchelor,Brenner)

$$\boldsymbol{\tau}^{\mathrm{NN}} = \boldsymbol{\tau}^{\mathrm{NN}}(\Psi) = \boldsymbol{\tau}^{\mathrm{NN}}(\langle \mathbf{nn} \rangle_{\Psi}, \langle \mathbf{nnnn} \rangle_{\Psi})$$

Non-Newtonian stress (Batchelor,Brenner)

$$\boldsymbol{\tau}^{\mathrm{NN}} = \boldsymbol{\tau}^{\mathrm{NN}}(\Psi) = \boldsymbol{\tau}^{\mathrm{NN}}(\langle \mathbf{nn} \rangle_\Psi, \langle \mathbf{nnnn} \rangle_\Psi)$$

$$\langle \mathbf{nn} \rangle_\Psi = \langle \mathbf{nn} \rangle_\Psi(\mathbf{x}, t) = \int_{\partial B(0;1)} \mathbf{nn}^T \ \Psi(\mathbf{x}, \mathbf{n}, t) \ \mathrm{d}\mathbf{n}$$

The model

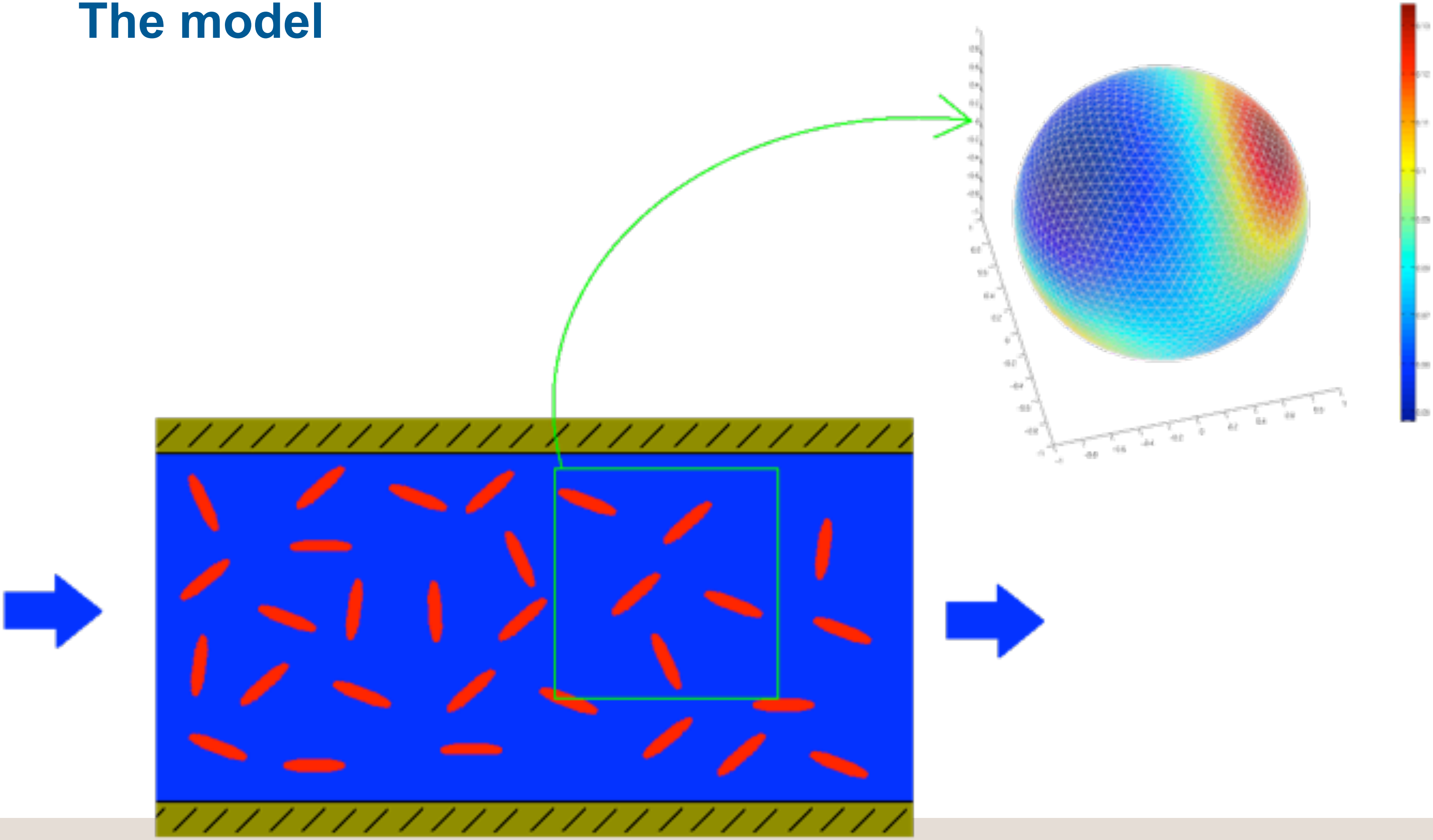

Previous approaches

- Monte-Carlo simulation (e.g. Manhart 2003)
- Moment closures (e.g. Shaqfeh 2005)
- Galerkin method with spherical harmonics (e.g. Gillissen 2007)

Novel Numerical Scheme

Novel Numerical Scheme

- Finite Volume Method (FVM)
- on a Triangular Geodesic Grid
- adaptivity to resolve local phenomena

Novel Numerical Scheme

- Finite Volume Method (FVM)
- on a Triangular Geodesic Grid
- adaptivity to resolve local phenomena

- conservative
- robust w.r.t. steep gradients
- allows for local adaptivity

TECHNISCHE UNIVERSITÄT MÜNCHEN

Geodesic grids

Geodesic grids

- Start with a platonic solid (e.g. icosahedron)

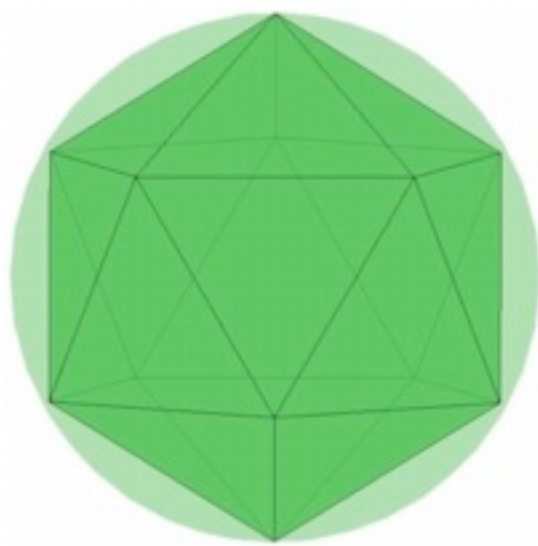

Geodesic grids

- Start with a platonic solid (e.g. icosahedron)
- Project the edges onto the circumscribed sphere

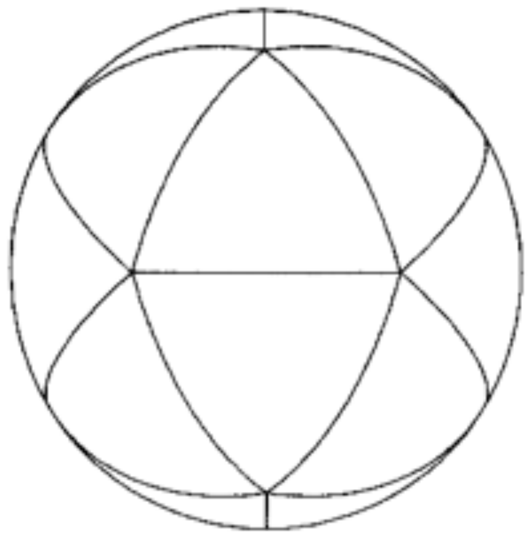

N = 1

Geodesic grids

- Start with a platonic solid (e.g. icosahedron)
- Project the edges onto the circumscribed sphere
- Refine (e.g. uniform refinement)

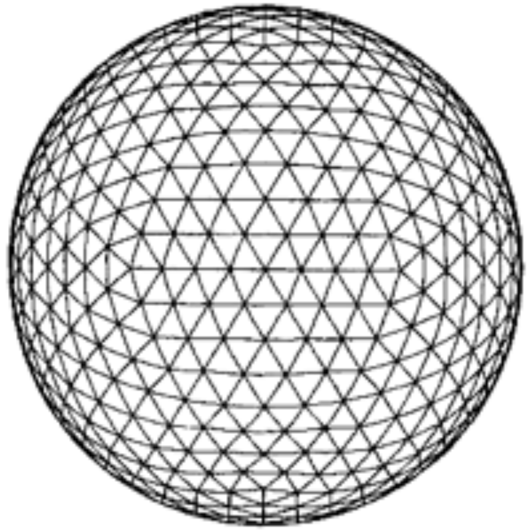

N = 8

TECHNISCHE UNIVERSITÄT MÜNCHEN

Geodesic grids (selected publications)

- Baumgardner (1985)
- Heikes & Randall (1995)
- Tomita et al (2001)
- Majewski et al (2002)
- Jablonowski (2004)
- Ahmad el al (2005)
- Ringler, Heikes, Randall (2005)
- Behrens (2005)
- Walko & Avissar (2008)

TECHNISCHE UNIVERSITÄT MÜNCHEN

Localized peak

Localized peak

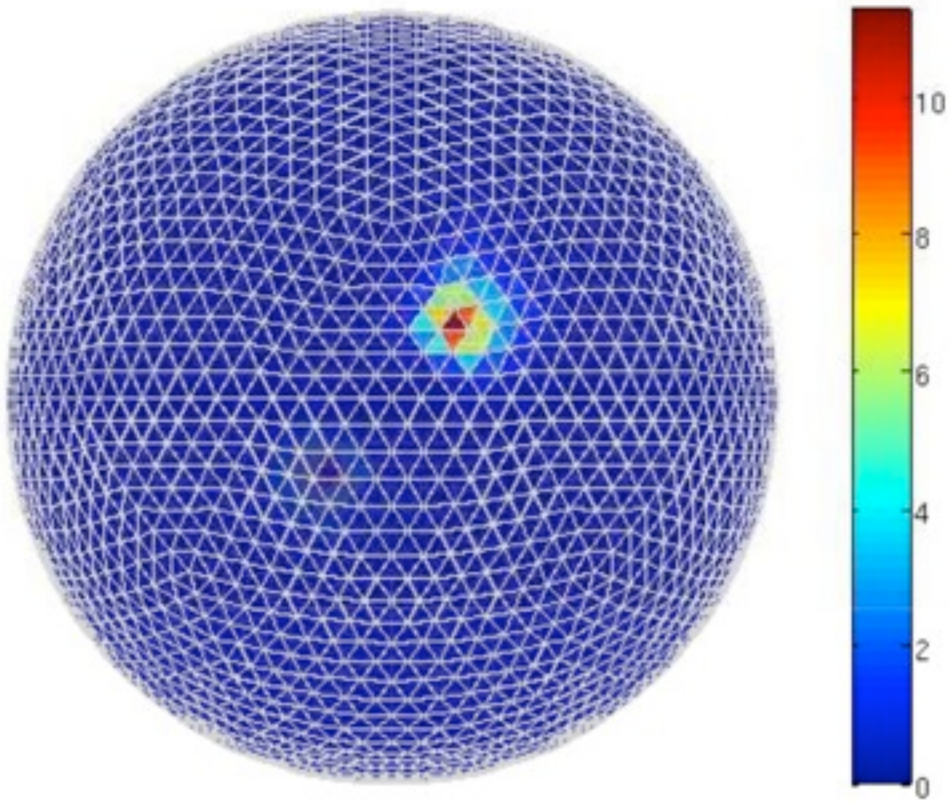

Localized peak

Idea: use high resolution only where required

Adaptivity

=> adaptivity

Adaptation method

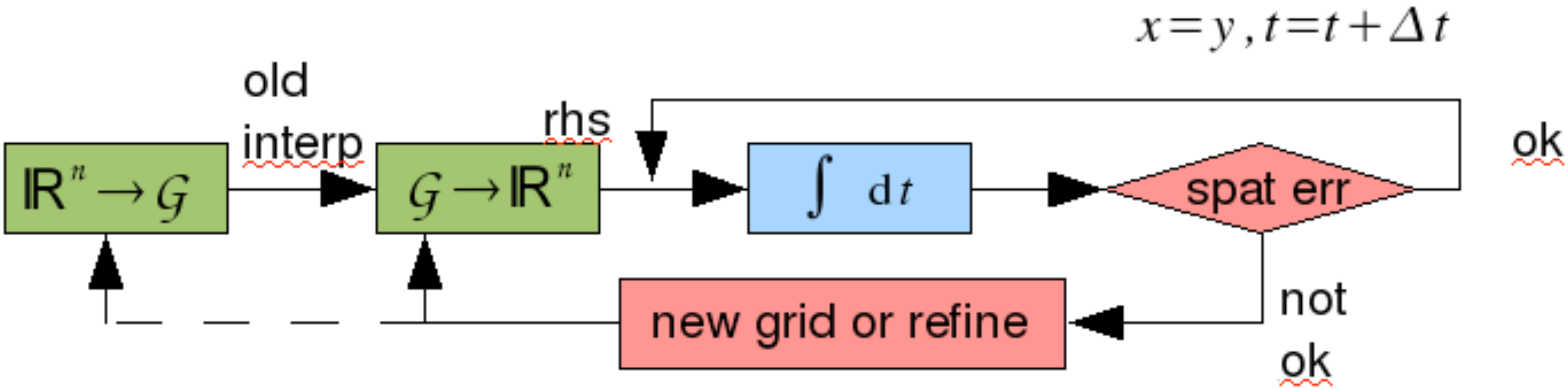

Analysis

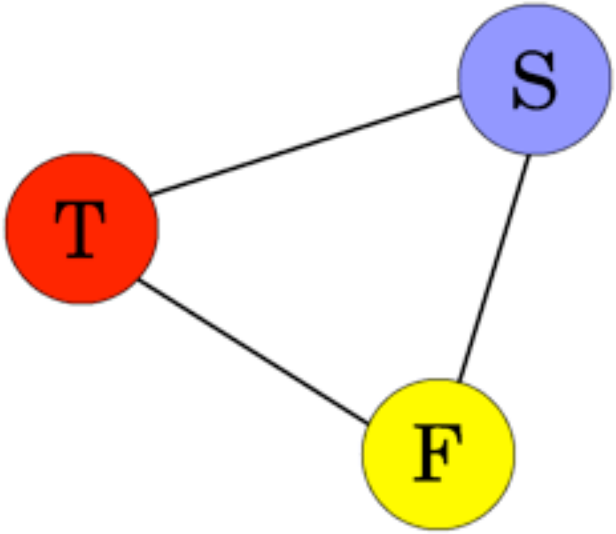

Analysis

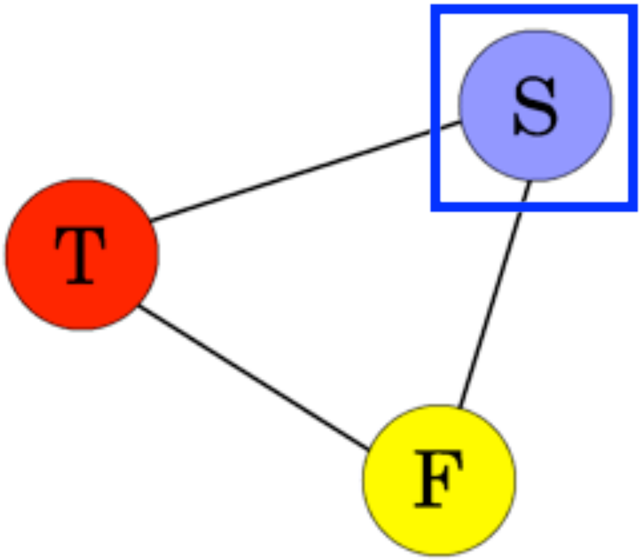

Goal

$$\boldsymbol{\tau}^{\mathrm{NN}} = \boldsymbol{\tau}^{\mathrm{NN}}(\Psi) = \boldsymbol{\tau}^{\mathrm{NN}}(\langle \mathbf{nn} \rangle_{\Psi}, \langle \mathbf{nnnn} \rangle_{\Psi})$$

$$\langle \mathbf{nn} \rangle_{\Psi} = \langle \mathbf{nn} \rangle_{\Psi}(\mathbf{x}, t) = \int_{\partial B(0;1)} \mathbf{nn}^{T} \; \Psi(\mathbf{x}, \mathbf{n}, t) \; \mathrm{d}\mathbf{n}$$

Control the goal quantity

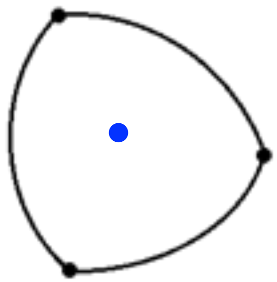

$$\langle \mathbf{nn} \rangle_{\Psi}^{h} \approx \langle \mathbf{nn} \rangle_{\Psi} + c_1 h^2$$

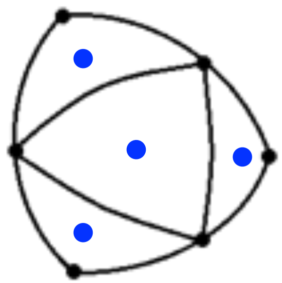

$$\langle \mathbf{nn} \rangle_{\Psi}^{\frac{h}{2}} \approx \langle \mathbf{nn} \rangle_{\Psi} + c_2 \frac{h}{2}^2$$

Control the goal quantity

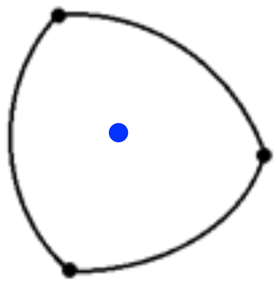

$$\langle \mathbf{nn} \rangle_{\Psi}^{h} \approx \langle \mathbf{nn} \rangle_{\Psi} + c_1 h^2$$

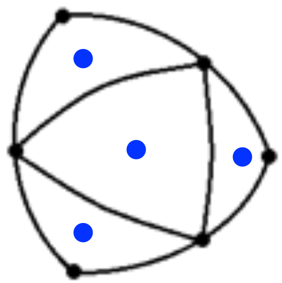

$$\langle \mathbf{nn} \rangle_{\Psi}^{\frac{h}{2}} \approx \langle \mathbf{nn} \rangle_{\Psi} + c_2 \frac{h}{2}^2$$

assume: $c_1 = c_2 =: c$

Control the goal quantity

$$\langle \mathbf{nn} \rangle_{\Psi}^{h} - \langle \mathbf{nn} \rangle_{\Psi}^{\frac{h}{2}} = c \left(h^2 - \frac{h^2}{4} \right) = \frac{3}{4} c h^2$$

$$= \frac{3}{4} c_1 h^2 =: \frac{3}{4} err_{\mathbf{nn}}$$

Behavior of the estimate

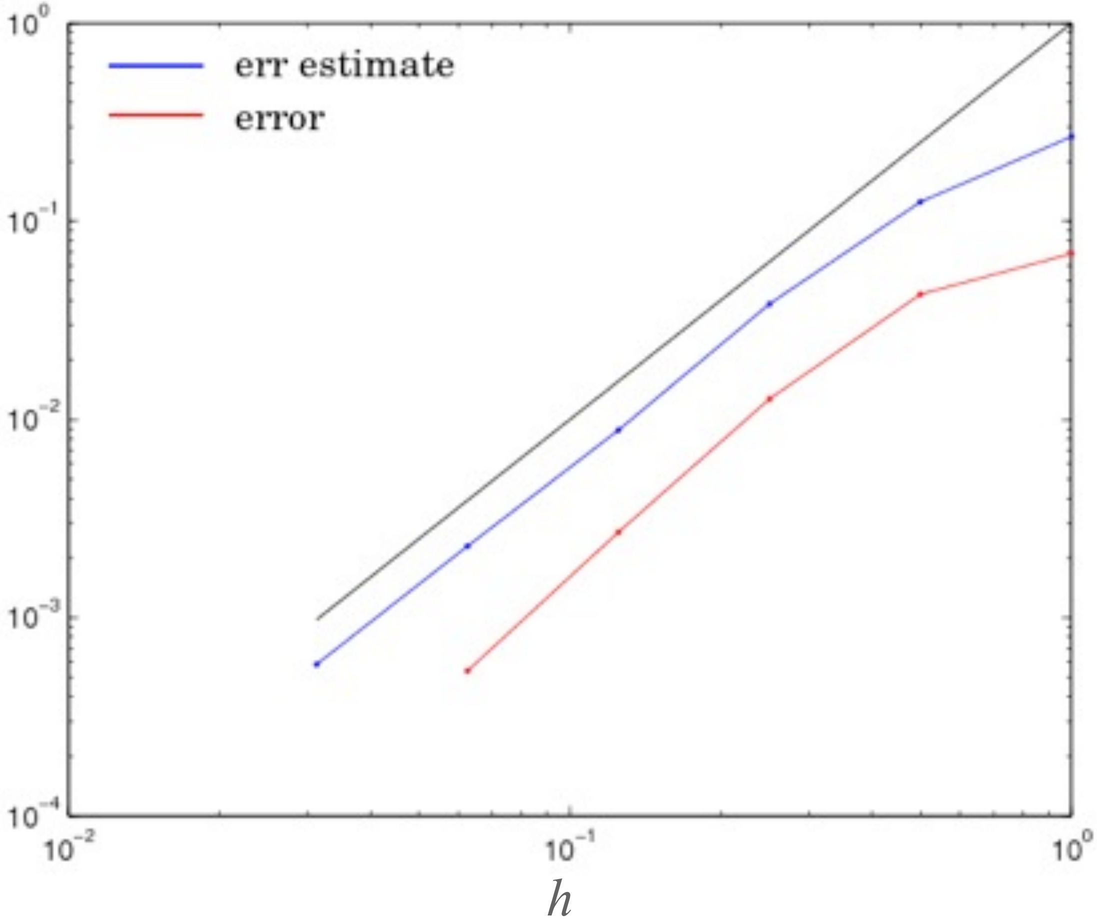

Analysis

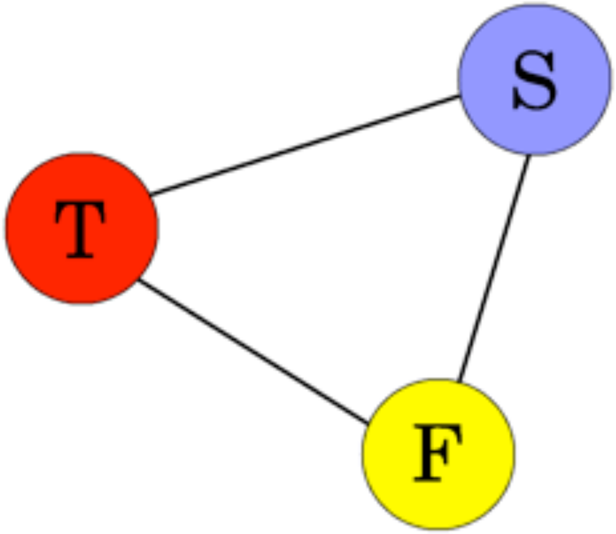

Analysis

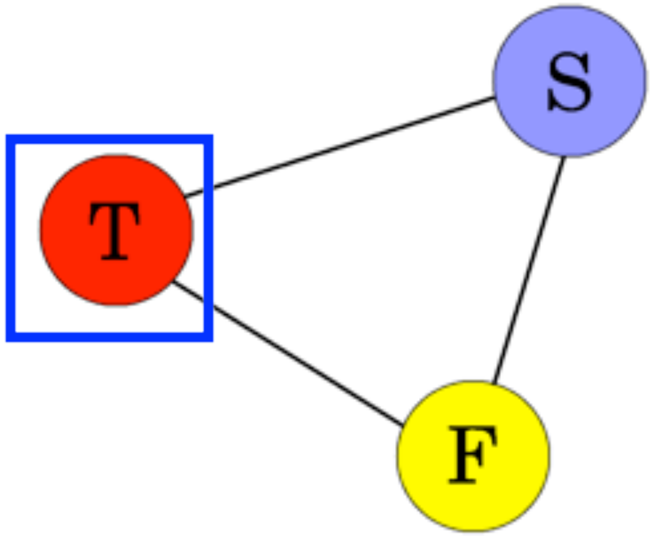

Eigenvalues

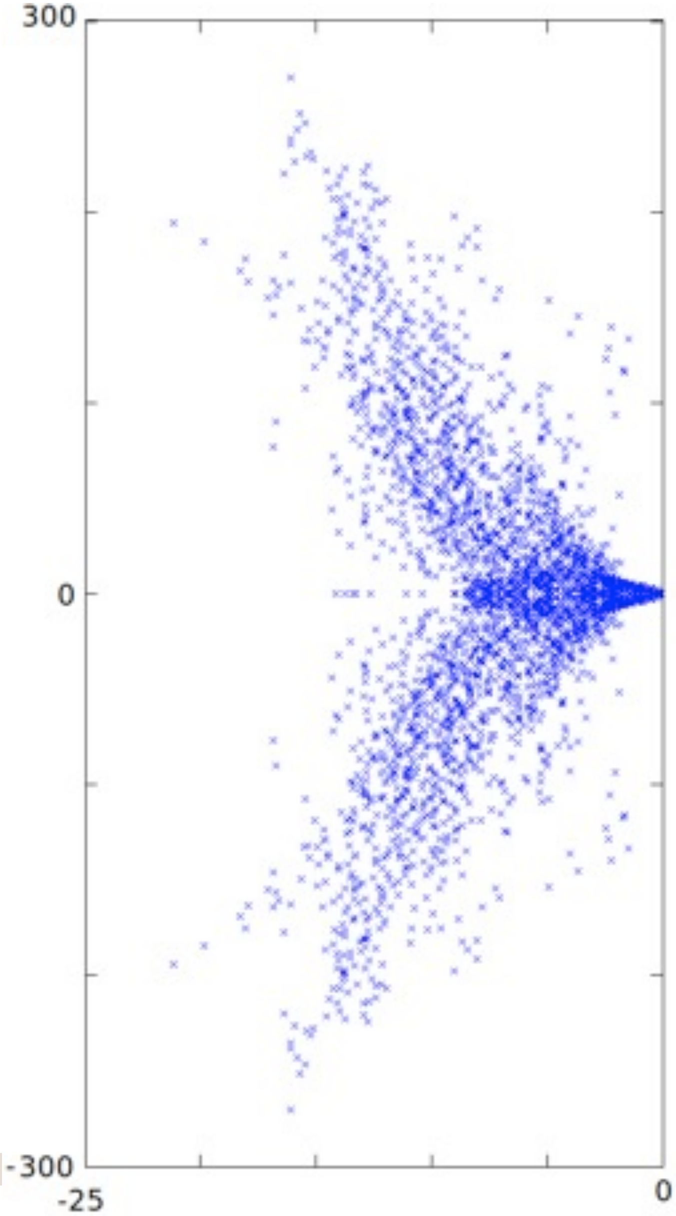

I-Stablity

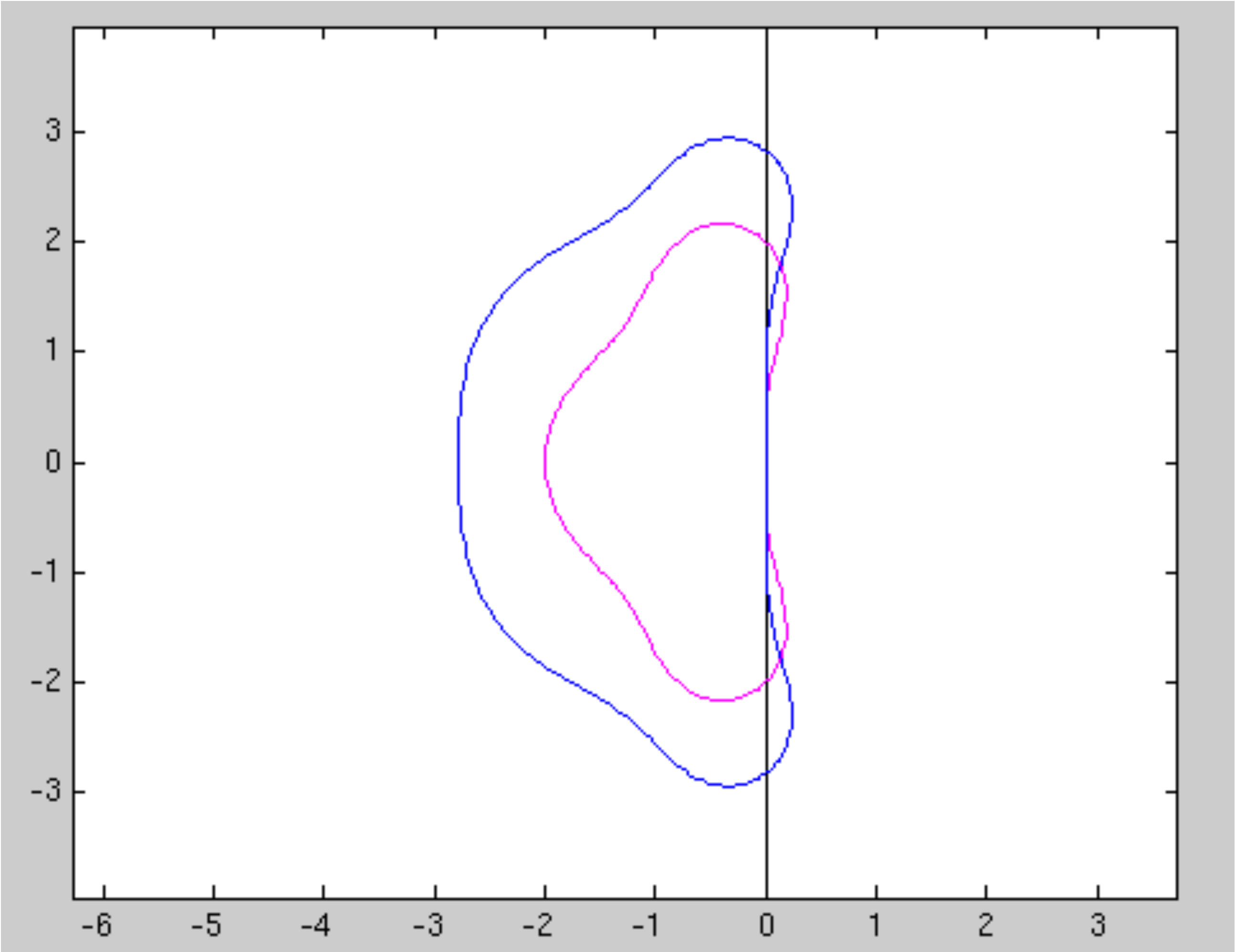

Analysis

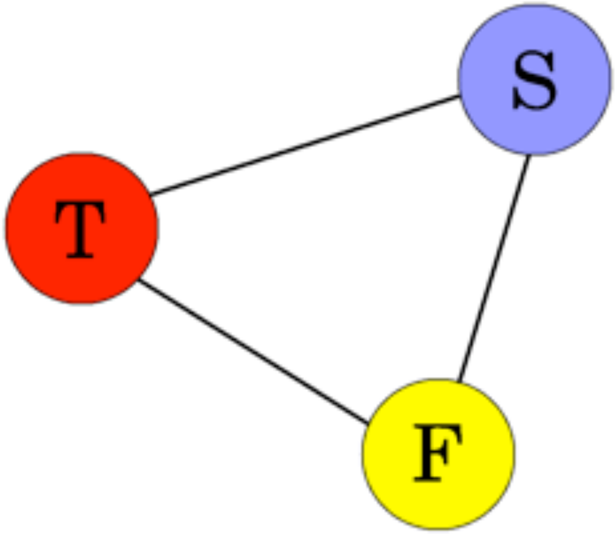

TECHNISCHE UNIVERSITÄT MÜNCHEN

Analysis

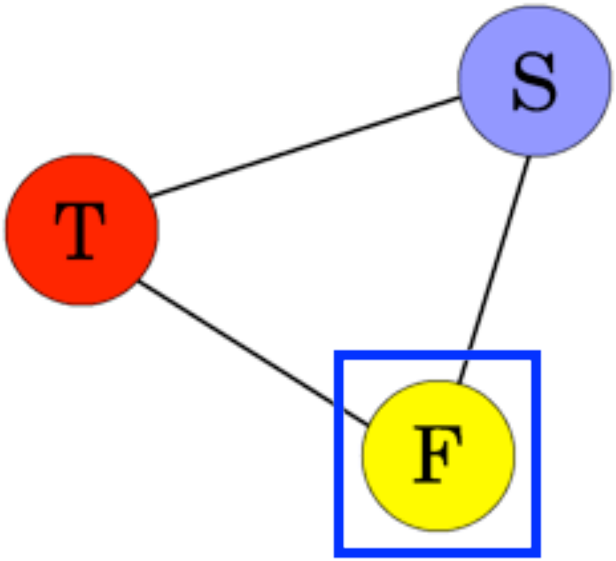

Blending

increased upwinding for edges with
hanging nodes

Adaptive mesh

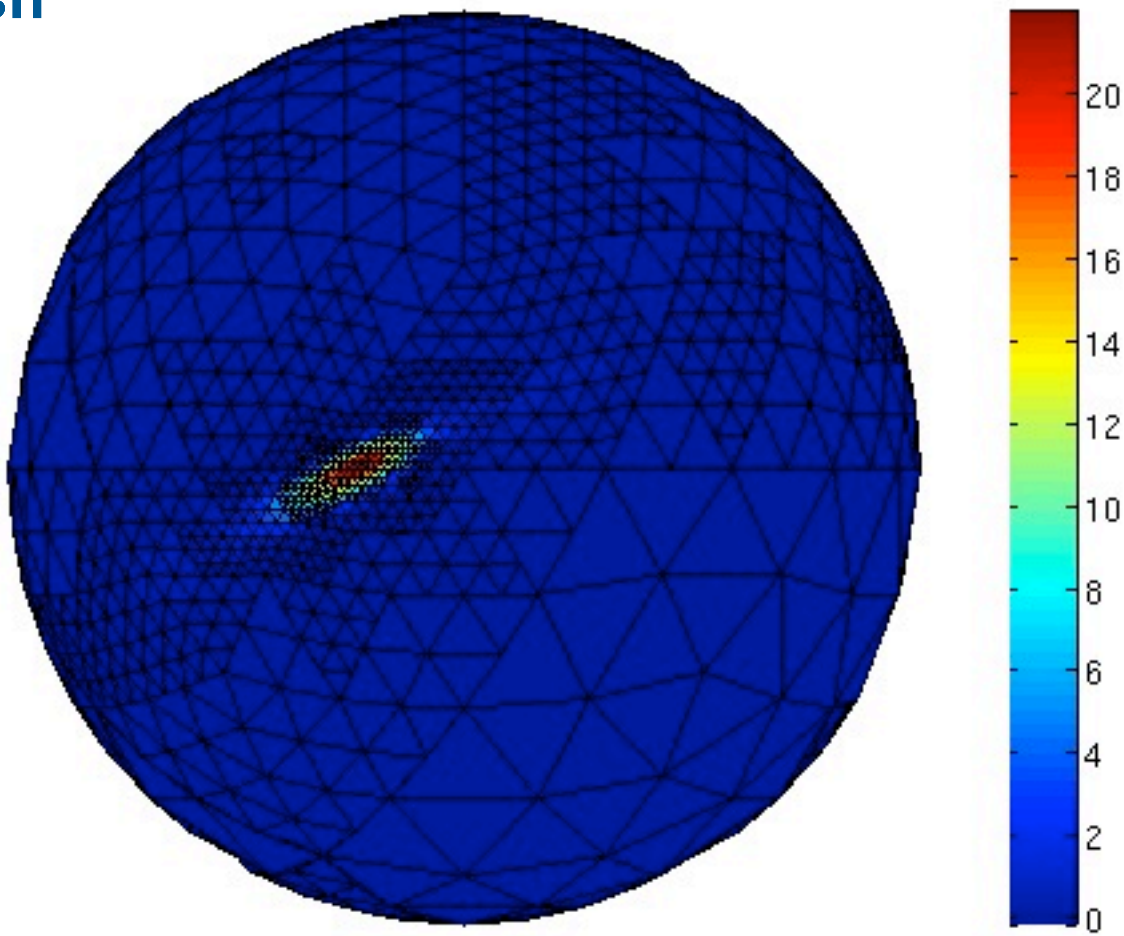

Results

Speed

Pe	solver	maximal grid level	average number of cells	CPU time (s)
98	MC	-	10 000 samples	2.39
	SH	-	50 modes	3.85
	FVM	3	640	2.86
	adaFoP (O2)	5	951	1.17
	adaFoP (RK4)	5	952	1.56
738	MC	-	10 000 samples	2.39
	SH	-	80 modes	15.83
	FVM	4	2560	14.46
	adaFoP (O2)	6	1110	1.68
	adaFoP (RK4)	6	1134	2.18

Table 2: Runtimes for the turbulent channel flow test case

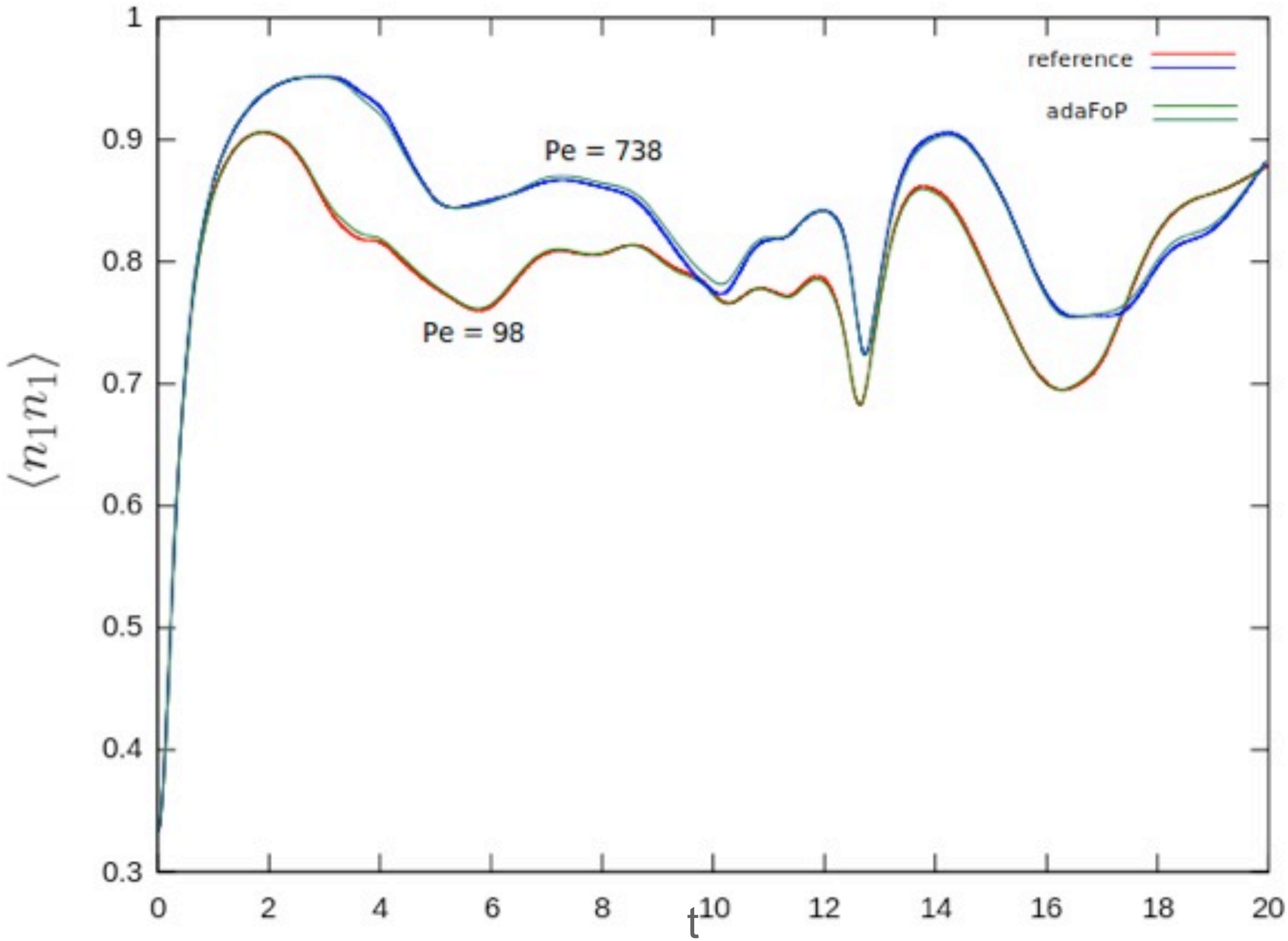
reference
adaFoP
Pe = 738
Pe = 98
$\langle n_1 n_1 \rangle$
t
1
0.9
0.8
0.7
0.6
0.5
0.4
0.3
0
2
4
6
8
10
12
14
16
18
20

Solution Quality

Pe	solver	L_1 in time	max in time	roughness
98	MC	$6.20 \cdot 10^{-2}$	$9.64 \cdot 10^{-2}$	$12.80 \cdot 10^{-3}$
	SH	$2.10 \cdot 10^{-2}$	$4.38 \cdot 10^{-2}$	$2.80 \cdot 10^{-3}$
	FVM	$8.53 \cdot 10^{-2}$	$1.15 \cdot 10^{-2}$	$6.70 \cdot 10^{-3}$
	adaFoP (O2)	$5.42 \cdot 10^{-2}$	$0.49 \cdot 10^{-2}$	$3.43 \cdot 10^{-3}$
	adaFoP (RK4)	$4.73 \cdot 10^{-2}$	$0.46 \cdot 10^{-2}$	$3.26 \cdot 10^{-3}$
738	MC	$4.75 \cdot 10^{-2}$	$0.88 \cdot 10^{-2}$	$6.08 \cdot 10^{-3}$
	SH	$2.30 \cdot 10^{-2}$	$0.88 \cdot 10^{-2}$	$1.72 \cdot 10^{-3}$
	FVM	$32.41 \cdot 10^{-2}$	$2.56 \cdot 10^{-2}$	$8.26 \cdot 10^{-3}$
	adaFoP (O2)	$10.22 \cdot 10^{-2}$	$1.08 \cdot 10^{-2}$	$6.01 \cdot 10^{-3}$
	adaFoP (RK4)	$9.91 \cdot 10^{-2}$	$1.16 \cdot 10^{-2}$	$5.83 \cdot 10^{-3}$

Acknowledgement

IGSSE TUM
International Graduate School of Science and Engineering

IGSSE Project 3-02
“Particle Dynamics in Turbulent Flows”

Team:
Prof. Manhart, Prof. Simeon, Dr. le Duc
A. Moosaie, E. Zharovsky

Showtime

movie

The End

Thank you for your attention!

Channel DNS